

Double Internal Bremsstrahlung in the Beta Decay of $Y^{90}\dagger$

P. S. JASTRAM AND J. C. VANDERLEEDEN*

Department of Physics, The Ohio State University, Columbus, Ohio 43210

(Received 24 April 1969)

The continuous coincidence γ -ray spectrum discovered in the process of searching for two-photon decay in Zr^{90} is found to be double inner bremsstrahlung originating in the 2.26-MeV β decay of Y^{90} to the Zr^{90} ground state. The angular correlation, energy dependence, and total transition intensity of the coincidence spectra are compared with recent theoretical calculations.

I. INTRODUCTION

DURING a search¹ for double-photon decay in the deexcitation of the 0^+ first excited state in Zr^{90} , a continuous photon-coincidence spectrum was observed that cannot be due to the expected two-photon decay (Fig. 1). In an attempt to determine the nature of these spectra, we have considered various explanations. Of these, the most likely one appeared to be that the continuous two-dimensional coincidence spectra are the result of double internal bremsstrahlung (DIB) originating in the intense $Y^{90} \rightarrow Zr^{90}$ 2.26-MeV β decay. The possibility that we were, in fact, observing DIB prompted Mulligan and Seyler² to carry out the calculation for this radiation process.

Single internal-bremsstrahlung (IB) photons are created when the nuclear charge is suddenly altered during β decay. The resulting photon spectrum is continuous, the intensity decreases rapidly with increasing energy, and the photon endpoint occurs at the β -spectrum endpoint. The intensity is Z independent in first approximation. The IB theory was worked out by Knipp and Uhlenbeck³ and by Bloch⁴ for allowed transitions, and extended by Chang and Falkoff⁵ and others^{6,7} to forbidden transitions. There is good agreement between theory and experiment regarding the intensity and shape of the IB spectrum, although recent work⁸ has shown the existence of a photon excess in electron-photon coincidence studies, near the upper endpoint of the spectrum.

In DIB, two photons are created in the same β decay. The DIB photons are in time coincidence, their energy distribution is continuous, and the endpoint of the photon sum-coincidence spectrum occurs at the β -spectrum endpoint. Whereas in IB the electron interacts with the radiation field only once, in DIB it interacts

twice. Therefore, one would expect the ratio of transition probabilities for DIB and IB to be on the order of α , where $\alpha = 1/137$, the fine structure constant. A simple classical argument shows that the angular dependence of the two coincident photons emitted in DIB favors the forward direction, and that this forward peaking will increase with increasing photon energy. An immediate consequence of this is that the angular-correlation anisotropy $\eta = W(180)/W(90)$ must be less than unity, which is indeed in accord with our experimental data.

The DIB has not been previously observed, although it has been investigated, both theoretically and experimentally, by Thun *et al.*⁹ Using a lens spectrometer, these investigators selected the energy of the β particle, and with two scintillation detectors placed at 90° to the spectrometer axis and 180° apart, they measured triple coincidences between the DIB photons and the electron. Whereas this method has the advantage of giving the DIB cross section as a function of electron energy, and while cosmic-radiation and accidental-coincidence rates are negligible, the energy selection and the coincidence requirement placed on the electron make the resulting triple-coincidence rate quite small. The outcome of Thun *et al.*'s work was inconclusive.

Mulligan and Seyler's differential cross section for DIB [Ref. 2, Eq. (10)] shows explicitly the dependence on the photon energies $E_\gamma(1)$ and $E_\gamma(2)$, on the energy of the β particle in the initial state and its momentum in the final state, and on the elements of solid angle into which the three particles are emitted.

In what follows we now compare the DIB theory with our experimental results. To this end, Mulligan and Seyler have numerically evaluated the total DIB spectrum for the 2.26-MeV β transition to the Zr^{90} ground state. Equation (10) in Ref. 2 was integrated over the β spectrum and over the momentum vector of the β particle in its final state. This calculation was carried out for various values of $E_\gamma(1)$ and $E_\gamma(2)$ such that $E_\gamma(1) + E_\gamma(2) = E$, for various values of E , and for five angles between the photon propagation vectors ($0^\circ, 45^\circ, 90^\circ, 135^\circ, 180^\circ$). For a simple comparison with theory, it is convenient to consider the ratio of the DIB and IB transition probabilities, since experimentally the IB spectrum can easily be measured. Therefore,

⁹ J. E. Thun *et al.*, Arkiv Fysik **22**, 565 (1962).

[†] For a preliminary account of this work see P. S. Jastram and J. C. Vanderleeden, Phys. Letters **19**, 29 (1965).

* Presently at the California Institute of Technology, Pasadena, Calif.

¹ J. C. Vanderleeden and P. S. Jastram, preceding paper, Phys. Rev. C **1**, 1025 (1970).

² B. Mulligan and R. G. Seyler, following paper, Phys. Rev. C **1**, 1041 (1970).

³ J. K. Knipp and G. E. Uhlenbeck, Physica **3**, 415 (1936).

⁴ F. Bloch, Phys. Rev. **50**, 272 (1936).

⁵ C. S. W. Chang and D. L. Falkoff, Phys. Rev. **76**, 365 (1949).

⁶ L. Madansky *et al.*, Phys. Rev. **84**, 596 (1951).

⁷ R. R. Lewis and G. W. Ford, Phys. Rev. **109**, 756 (1957).

⁸ B. Persson, Nucl. Phys. **67**, 121 (1965).

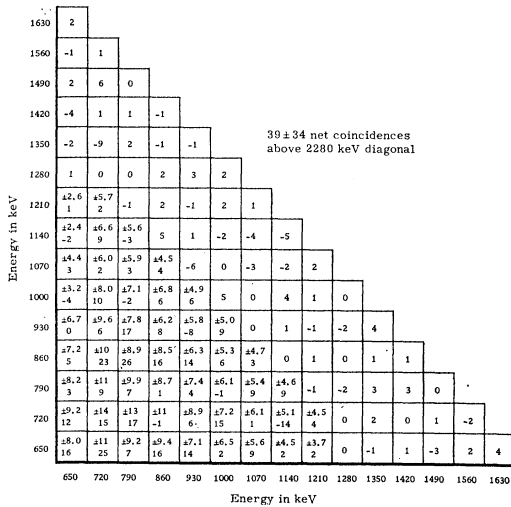
Knipp and Uhlenbeck's expression³ for IB was also evaluated for the same values of E as were used in the DIB calculation.

II. DATA ANALYSIS

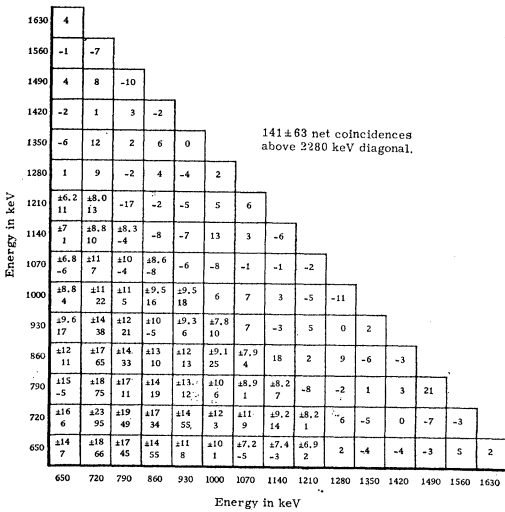
If the incident (singles) IB spectrum is specified by the probability that the energy lies between E and $E+dE$, $W_{IB}(E)dE$, then the singles counting rate at a pulse height corresponding to energy E_α in a window of width $\Delta E=70$ keV, is given by

$$C_{IB}(E_\alpha) = K \int_0^{E_{\max}} W_{IB}(E) \rho_1(E_\alpha, E) \Delta E, dE. \quad (1)$$

Here $\rho_1(E_\alpha, E)$ is the scintillation-counter response



(a)



(b)

FIG. 1. Net two-dimensional photon coincidence spectra, observed in the $Sr^{90} \rightarrow Y^{90} \rightarrow Zr^{90} \beta$ decay. (a) 180° data accumulated in 324 h and (b) 90° data accumulated in 600 h.

function, representing the probability that a photon with energy E produces a pulse with amplitude corresponding to E_α . Also, K is a constant characteristic of the source strength. Since the incident photon spectrum $W_{IB}(E)$ drops off quite rapidly with increasing energy, we set in good approximation

$$C_{IB}(E_\alpha) \sim K W_{IB}(E_\alpha) \rho_1(E_\alpha, E_\alpha) \Delta E, \quad (2)$$

where $\rho_1(E_\alpha, E_\alpha) \Delta E$ now represents the counter-efficiency factor for detection of a photon with energy E_α in a window of width $\Delta E=70$ keV, centered at the photopeak.

The validity of the approximation in Eq. (2) is supported by the work of Persson¹⁰ who made an accurate measurement of the IB spectrum shape in P^{32} and Y^{90} . Using smaller scintillation crystals than ours (with a subsequent smaller photo fraction) he finds that the *measured* and *incident* IB spectra differ by only $\sim 10\%$ above 1 MeV and by less below 1 MeV.

The analysis of the DIB spectrum is carried out in analogy with the preceding development for IB. If $C_{DIB}(E_{i,j})$ is the DIB coincidence counting rate in the (i,j) element of the two-dimensional spectrum, and if $W_{DIB}(E_{i,j}) \Delta E \Delta E$ stands for the probability that the two photon energies fall within the (i,j) element, then

$$C_{DIB}(E_{i,j}) \sim K W_{DIB}(E_{i,j}) \rho_1(E_i, E_i) \rho_2(E_j, E_j) \Delta E \Delta E. \quad (3)$$

When we let $C_{DIB}(E_\alpha)$ represent the total DIB counting rate on the diagonal with sum energy E_α (i.e., $E_i + E_j = E_\alpha$), then

$$C_{DIB}(E_\alpha) \equiv \sum_{i+j=\alpha} C_{DIB}(E_{i,j}) \sim K \times \sum_{i+j=\alpha} W_{DIB}(E_{i,j}) \rho_1(E_i, E_i) \rho_2(E_j, E_j) \Delta E \Delta E, \quad (4)$$

where the summation is limited to the elements above the 650-keV lower discriminator cutoffs. As a further approximation we set

$$\rho_1(E_i, E_i) \rho_2(E_j, E_j) \Delta E \Delta E \sim [\rho(\frac{1}{2}E_\alpha, \frac{1}{2}E_\alpha) \Delta E]^2,$$

i.e., on a given diagonal sum the product of the counter response functions is considered to be constant. This is a reasonable approximation, since ρ_1 increases and ρ_2 decreases (or *vice versa*) when traversing a diagonal, while also the counters and their geometries are identical. Then, upon introducing the notation

$$\sum_{i+j=\alpha} W_{DIB}(E_{i,j}) \equiv W_{DIB}(E_\alpha),$$

Eq. (4) becomes

$$C_{DIB}(E_\alpha) \sim K W_{DIB}(E_\alpha) [\rho(\frac{1}{2}E_\alpha, \frac{1}{2}E_\alpha) \Delta E]^2. \quad (5)$$

¹⁰ B. Persson, Nucl. Phys. **55**, 49 (1964).

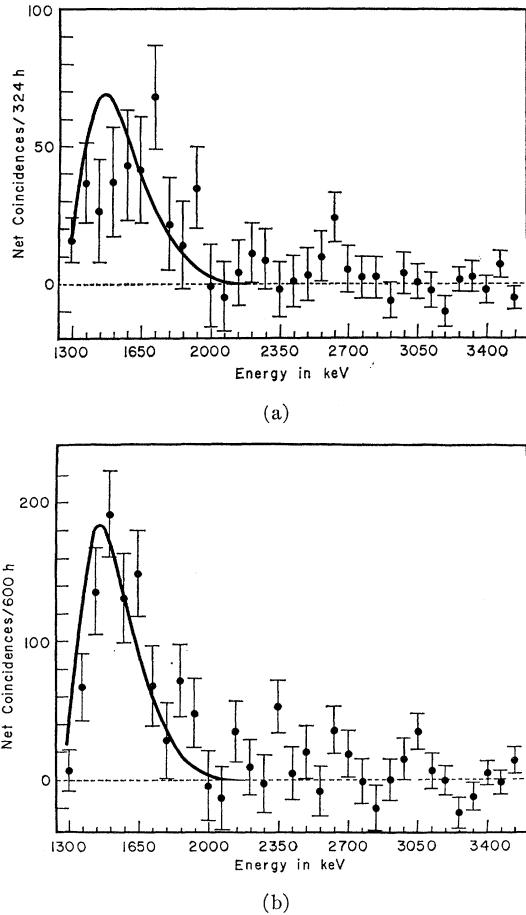


FIG. 2. Net coincidences versus diagonal-sum energy for (a) the 180° data and (b) the 90° data. The peaks at about 1650 keV are instrumental in origin: the diagonal sum extends over fewer elements at lower sum energies. Both spectra appear to approach a 2280-keV endpoint, but weak high-energy tails extend beyond that. The solid line is a fit to the DIB theory of Mulligan and Seyler.

Solving Eqs. (2) and (5) for $W_{\text{DIB}}(E_\alpha)/W_{\text{IB}}(E_\alpha)$ gives

$$\frac{W_{\text{DIB}}(E_\alpha)}{W_{\text{IB}}(E_\alpha)} \sim \frac{C_{\text{DIB}}(E_\alpha)}{C_{\text{IB}}(E_\alpha)} \left(\frac{\rho(E_\alpha, E_\alpha) \Delta E}{\{\rho(\frac{1}{2}E_\alpha, \frac{1}{2}E_\alpha) \Delta E\}^2} \right). \quad (6)$$

The quantity in the large parentheses is calculated from the counter response functions which were obtained using National Bureau of Standards calibrated γ -ray sources. $C_{\text{IB}}(E_\alpha)$ is calculated from a Sr^{90} singles IB spectrum (not shown). The quantities $C_{\text{DIB}}(E_\alpha)$ are obtained by summing the two-dimensional spectra (Fig. 1) over diagonals $E_\gamma(1) + E_\gamma(2) = E$, and plotting the resulting sum against E (see Fig. 2; the solid line is a theoretical fit, to be commented upon shortly). The results are shown in Fig. 3(a) (180° data) and Fig. 3(b) (90° data), where $W_{\text{DIB}}(E_\alpha)/W_{\text{IB}}(E_\alpha)$ is plotted as a function of E_α . The solid lines represent the theoretical result of Mulligan and Seyler.

The directional correlation of the DIB photons

[Ref. 2, Eq. (10)] turns out to be forward peaked, the peaking increasing with increasing photon energy. The theoretical anisotropy,¹¹ averaged over the diagonal-sum energy E_α from 1300 to 2280 keV is

$$\begin{aligned} \eta_{\text{DIB}} &= \langle W(180)/W(90) \rangle_{\text{DIB}} \\ &\equiv \sum_{\alpha} W_{\text{DIB}}^{180}(E_\alpha) / \sum_{\alpha} W_{\text{DIB}}^{90}(E_\alpha) \quad (7) \\ &= 0.445. \quad (7') \end{aligned}$$

Experimentally, the anisotropy is calculated by solving Eq. (5) for $W_{\text{DIB}}(E_\alpha)$, and averaging over the same values of E_α as in the theoretical calculation:

$$\begin{aligned} \eta_{\text{expt}} &= \left\langle \frac{\bar{W}(180)}{\bar{W}(90)} \right\rangle_{\text{expt}} \\ &\equiv \frac{\sum_{\alpha} C_{\text{DIB}}^{180}(E_\alpha) / [\rho(\frac{1}{2}E_\alpha, \frac{1}{2}E_\alpha) \Delta E]^2}{\sum_{\alpha} C_{\text{DIB}}^{90}(E_\alpha) / [\rho(\frac{1}{2}E_\alpha, \frac{1}{2}E_\alpha) \Delta E]^2} \quad (8) \\ &= 0.74 \pm 0.18. \quad (8') \end{aligned}$$

This result must be adjusted downward by an estimated 10% to account for the finite angular resolution of the detectors. The anisotropy is averaged over the sum energy E_α , rather than displayed graphically by plotting against E_α , since poor statistics on the individual points make a meaningful comparison difficult.

Returning to Fig. 2, we have also fitted the theoretical diagonal-sum spectra to our experimental data by requiring that the total area under the theoretical curve be equal to the total number of coincidences up to the 2.28-MeV diagonal sum. The theoretical result is represented by the solid curve.

III. DISCUSSION

The preceding analysis of our data in terms of double internal bremsstrahlung has shown the following:

(a) Over all, the experimental diagonal-sum spectra (Fig. 2) are satisfactorily fitted by the theoretical curves. However, deviations from a good fit to occur, particularly near the theoretical DIB endpoint (2.26 MeV).

(b) The experimental value of the angular-correlation anisotropy, when corrected for the finite angular resolution of the detectors, differs by about $1\frac{1}{2}$ standard deviations (about 25%) from the theoretical value. Some attenuation of the anisotropy will result from Compton scattering from the steel collimator.

(c) Both the energy dependence and the magnitude of the ratio of transition probabilities for DIB and IB, $W_{\text{DIB}}/W_{\text{IB}}$, are in good agreement with theory (Fig. 3).

¹¹ The values given here for the theoretical and experimental angular correlation anisotropy differ from those in Ref. 1; this is due to the use of an improved computer program and elimination of a numerical error in the experimental value.

Although the experimental data fit the DIB hypothesis, the results summarized in (a), (b) and (c) represent convincing evidence for the observation of DIB only if alternative interpretations of our data are either quite unlikely or can be rejected altogether. There are several well known processes (such as counter-to-counter Compton scattering) that produce continuous coincidence spectra similar to the ones observed. These questions are considered in detail in Appendix A, along with the results of the relevant measurements and checks. We conclude that the experimental coincidence spectra are primarily due to source-originating coincident photons with a continuous energy distribution, and that neither source impurities nor instrumental distortions can account for our data.

In view of the above conclusions and considering the satisfactory fit of our data to the DIB theory of Mulligan and Seyler, we attribute the continuous photon-coincidence spectrum observed in the $\text{Sr}^{90} \rightarrow \text{Y}^{90} \rightarrow \text{Zr}^{90}$

decay to double internal bremsstrahlung arising in the 2.26-MeV β transition to the Zr^{90} ground state.

ACKNOWLEDGMENTS

We thank Dr. R. G. Seyler and Dr. B. Mulligan for their interest in this work, in particular for developing the theory of double internal bremsstrahlung and for programming the particular calculations of interest to us.

APPENDIX A

1. Undersubtraction

An obvious first test is to ascertain that the coincidence spectra are not due to undersubtraction of accidental and/or cosmic-radiation coincidences. To this end, one of the scintillation counters was removed from the cosmic-radiation shield and viewed a Zn^{65} source (511-keV and 114-keV photons), while the counter remaining in the shield detected the 842-keV photons of Mn^{54} . Singles rates were adjusted to equal those obtained with the Sr^{90} source. In this arrangement, true coincidences are not possible, and subtraction of delayed from prompt coincidences must yield zero. This it did; the "excess" counts of one typical run was -15 ± 31.6 coincidences/20 h.

2. Compton Scattering—Pile Up Events

Consider the situation in which a photon is Compton scattered in one counter and detected in the other counter. The fast coincidence circuit (FCC) will respond to such events, but the discriminator setting of the intermediate resolution coincidence circuit (ICC), 600 keV, and of the pulse-height analyzer (PHD), 650 keV, prevent these events from being detected in either the 90° or the 180° counter configuration. Specifically, for primary photon energies above about 850 keV, the energy of the scattered photon which is detected in the second counter is about 200 keV when the counters are 90° apart. Thus the amplitude condition in channel 1 has been met, and the FCC has responded (it responds to all pulses above ~ 125 keV). However, the channel-2 PHD has not responded, nor has the channel-2 fast discriminator in the ICC; yet, if a pile-up event takes place in the second counter within the time resolution of the ICC¹² (~ 100 nsec), these conditions may be met and a coincidence recorded.

This contribution to the total coincidence rate was determined by recording the counter-to-counter Compton scattering rate with a Mn^{54} source, with the lower discriminators in the PHD's and the ICC moved down to 125 keV for both the 90° and 180° detector configuration. With the aid of the known singles rates, the Comp-

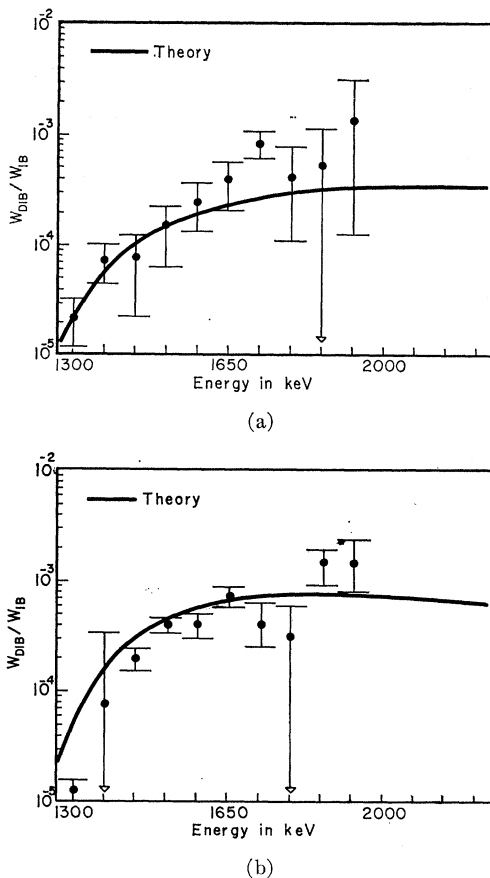


FIG. 3. Probability for production of two internal-bremsstrahlung photons in the same β decay and with sum energy E , divided by the probability for production of the internal-bremsstrahlung photon with energy E , plotted versus E . The heavy line is the theoretical result of Mulligan and Seyler for the 2.26-MeV β decay from Y^{90} to the Zr^{90} ground state. (a) Shows the 180° data and (b) the 90° data.

¹² It may be observed that, had the ICC not been used in this experiment, this pile-up event could be allowed to occur within the pulse resolution of the linear amplifiers in the PHD ($\sim 1 \mu\text{sec}$), resulting in a Compton-scattering pile-up rate ~ 10 times as high.

ton scattering pile-up rate was calculated for the Sr⁹⁰ continuous bremsstrahlung spectrum, and found to account for less than 1% of the 90° coincidence spectrum and less than 0.03% of the 180° spectrum (the lead-tantalum absorbers on the detectors greatly reduce the backscattering rate at 180°).

3. Higher-Order Accidentals

This anticipated contribution to the net coincidence rate had prompted us to modify the spectrometer by the inclusion of the ICC, as discussed in the preceding article. With a knowledge of the Sr⁹⁰ fast-coincidence rate with the ICC in operation, the Sr⁹⁰ singles rates, and the resolution of the slow coincidence circuits ($2\tau \sim 2 \mu\text{sec}$), term A_1 of the total accidental rate was calculated.¹³ This term involves chance events in the slow coincidence circuits. We find that A_1 accounts for less than 0.01% of the observed coincidence spectra. Had the ICC not been used, this contribution would be $\sim 4.5\%$ in the 180° spectrum and less in the 90° spectrum.

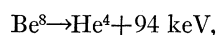
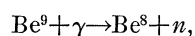
As another example of the effects that have been considered, cosmic-radiation coincidences which do not satisfy the pulse-height conditions in one or both channel(s), might still contribute to the prompt coincidence rate when photons emitted by the Sr⁹⁰ source satisfy the pulse-height requirements within the resolution of the ICC. As these photons are not present during a cosmic-background run, a coincidence excess could be produced. Calculations showed this contribution to be negligible.

4. Coincidence Rate as a Function of Source Separation

Singles counting rates and coincidences were recorded for some time with the counters at a slightly larger distance ($3\frac{1}{4}$ in. versus $2\frac{1}{4}$ in.) from the source than in the original runs. Letting $\alpha = (\text{new singles rate}) / (\text{original singles rate})$, we find that the net coincidence rate under the new conditions is α^2 times the original rate. Only true coincidences, originating in the source or its immediate environment, could lead to this result.

5. Source-Induced Short-Lived Activity

Such short-lived activities can add to the coincidence rate during a source run, dying out rapidly to produce a negligible contribution during the subsequent cosmic-radiation run. In the present case, the only reaction energetically allowed is a bremsstrahlung-induced photonuclear reaction on the beryllium source holder,



which clearly cannot account for the experimental data.

¹³ E. B. Shera, K. J. Casper, and B. L. Robinson, Nucl. Instr. Methods **24**, 482 (1963).

6. Radioactive Contaminant

The continuous nature of the two-dimensional coincidence spectra is reasonably well established, considering the size of the standard deviations, in that there are no localized "hot spots" as might be produced by the photopeak response of a γ -ray cascade in a contaminant. To check against possible spectrum distortion and to ascertain the pulse-height resolution of the spectrometer, we have verified that a true γ -ray cascade would indeed produce observable "hot spots." Coincidences were accumulated with a weak Co⁶⁰ source; coincidence peaks at the (1.173 MeV, 1.332 MeV) and (1.332 MeV, 1.173 MeV) positions stood out clearly, with a full width at half-maximum of about one matrix element (70 keV), even when the number of counts in the peak, and statistics, were comparable to those in the Sr⁹⁰ coincidence spectra. It is unlikely then that γ -ray cascades (as in a contaminant) account for the bulk of the observed coincidences, although the possibility of a small contribution cannot be discounted. In particular, the slight excess of coincidences above the 2.28-MeV diagonal sum (Fig. 2) might be due to a source impurity, in which case there may be a contribution to the continuum below the 2.28-MeV diagonal sum as well. The magnitude of this is estimated by extrapolating the high-energy tail below 2.28 MeV and comparing the area under it with the total area below 2.28 MeV. This leads to $\sim 15\%$ for the possible contribution of a contaminant.

7. Internal-External Bremsstrahlung Coincidence

A continuous external bremsstrahlung (EB) spectrum is produced in radiative scattering of β particles in the Coulomb field of nuclei other than the one in which the β decay originates.¹⁴ This photon spectrum has an endpoint equal to the β -spectrum endpoint, and the thick-target yield $\propto Z$ for β energies up to a few MeV.¹⁵

Internal-external bremsstrahlung coincidences can now occur when the first IB photon is created in the β decay, while the second EB photon is produced by the same β particle in the Be source holder. The two photons are in time coincidence and the endpoint of the energy sum-coincidence spectrum will be equal to the β -spectrum endpoint. We have made a rough calculation of the expected rate for IB-EB coincidences, created in and by the Y⁹⁰ \rightarrow Zr⁹⁰ 2.26-MeV β decay, and find that this process can account for no more than about 1% of our experimental data.

8. Summary

The majority of the observed coincidences are the result of a source-originating phenomenon of which

¹⁴ W. Heitler, in *The Quantum Theory of Radiation* (Oxford University Press, London, 1954), 3rd ed., p. 242 ff.

¹⁵ See for instance, R. D. Evans, *The Atomic Nucleus* (McGraw-Hill Book Co., New York, 1955), Chap. 21.

possibly as much as 15% might be the result of a source impurity; higher order accidentals cannot account for more than $\sim 1\%$; and double-photon decay (see Ref. 1) contributes a maximum of $\sim 15\%$. Furthermore, the coincident incident photon spectrum must be fairly continuous.

APPENDIX B

A particularly favorable case for the detection of DIB would seem to be the $P^{32} \rightarrow S^{32} \beta$ decay, which is an allowed transition with an endpoint energy of 1.71 MeV. We have taken data with a P^{32} source that at the start had an activity of about 2 mC. Coincidences were

recorded at 180 and 90°, for a total of 100 h each, and with the lower discriminators moved down to 545 keV. The results, however, were inconclusive. The net diagonal-sum coincidence spectra do not approach an endpoint at 1.71 MeV, but extend beyond it, and the calculated values of $W_{DIB}(E_\alpha)/W_{IB}(E_\alpha)$ are roughly three to five times larger than the theoretical values. Also, theoretically we should find for the anisotropy, averaged over energy from 1160 to 1720 keV, $\eta_{DIB} = 0.573$. This compares with an experimental value of 0.83 ± 0.37 . These discrepancies were thought to be due to a radioactive contaminant in the P^{32} source. Later tests verified this, showing the presence of Ag^{110} .

Beta-Gamma-Gamma Direction-Correlation Function for Two-Photon Radiation Emitted During Allowed Beta Decay

B. MULLIGAN AND R. G. SEYLER

Department of Physics, The Ohio State University, Columbus, Ohio 43210

(Received 24 April 1968)

Two Feynman diagrams for double internal bremsstrahlung are evaluated for an allowed β decay. The nucleons are treated nonrelativistically, and Coulomb effects are not considered.

1. INTRODUCTION

THE process of internal bremsstrahlung (IB), where a photon is emitted during the β decay of a nucleus, was first observed by Aston¹ in 1927. The classic theoretical studies of IB were published by Knipp and Uhlenbeck² and by Block³ in 1936.

Occasionally, two photons should be emitted during β decay. This double internal bremsstrahlung (DIB) process should occur with a probability per β decay of order α^2 , where $1/\alpha \approx 137$.

Recently, Jastram and Vanderleeden⁴ observed a continuous two-photon coincidence spectrum in the β decay of Y^{90} . The question of whether they were observing DIB provided the impetus for the present calculation of the general DIB β - γ - γ direction-correlation function.

In the only previously published DIB calculation, that of Thun *et al.*,⁵ the authors restrict themselves to that special case in which the electron is emitted in a direction perpendicular to two oppositely directed pho-

tons. We have verified that when applied to this special case our result agrees with theirs.

2. DERIVATION OF THE CORRELATION FUNCTION

In Fig. 1, we present the DIB Feynman diagrams to be considered. Assuming an *allowed* β decay, treating the nucleons nonrelativistically, and adopting the set of units in which $c = \hbar = m_e = 1$, we evaluate the diagrams of Fig. 1. Employing standard techniques,⁶ we quickly deduce the following expression for the differential probability $dP_{\beta\gamma\gamma}$ of the emission of an anti-neutrino of energy q whose direction and polarization are unspecified, and an electron and two photons, of energy E , k_1 , and k_2 , respectively, of direction specified by the solid angles $d\Omega_e$, $d\Omega_1$, and $d\Omega_2$, respectively, but of unspecified polarization:

$$dP_{\beta\gamma\gamma} = dk_1 dk_2 dE d\Omega_1 d\Omega_2 d\Omega_e \alpha^2 P_\beta(E + k_1 + k_2) F \\ \times \sum_{\text{pol}} \frac{1}{4} \text{Tr}[T\gamma_4 T'(p+1)] \\ = dP_{\beta\gamma\gamma}(q; p, \Omega_e; k_1, \Omega_1; k_2, \Omega_2), \quad (1)$$

¹ G. H. Aston, Proc. Cambridge Phil. Soc. **22**, 935 (1927).

² J. K. Knipp and G. E. Uhlenbeck, Physics **3**, 425 (1936).

³ F. Block, Phys. Rev. **50**, 272 (1936).

⁴ P. S. Jastram and J. C. Vanderleeden, Phys. Letters **19**, 29 (1965).

⁵ J. E. Thun, W. D. Hamilton, K. Siegbahn, and K. E. Eriksson, Arkiv Fysik **22**, 55 (1962).

⁶ S. DeBenedetti, in *Nuclear Interactions* (John Wiley & Sons, Inc., New York, 1964), Chap. 6.